Spinal Cord Modular Organization and Rhythm Generation: An NMDA Iontophoretic Study in the Frog

PHILIPPE SALTIEL, MATTHEW C. TRESCH, AND EMILIO BIZZI
Department of Brain and Cognitive Sciences, Massachusetts Institute of Technology, Cambridge, Massachusetts 02139

Saltiel, Philippe, Matthew C. Tresch, and Emilio Bizzi. Spinal cord modular organization and rhythm generation: a NMDA iontophoretic study in the frog. *J. Neurophysiol.* 80: 2323–2339, 1998. Previous work using electrical microstimulation has suggested the existence of modules subserving limb posture in the spinal cord. In this study, the question of modular organization was reinvestigated with the more selective method of chemical microstimulation. *N*-methyl-D-aspartate (NMDA) iontophoresis was applied to 229 sites of the lumbar spinal cord gray while monitoring the isometric force output of the ipsilateral hindlimb at the ankle. A force response was elicited from 69 sites. At 18 of these sites, tonic forces were generated and rhythmic forces at 44. In the case of tonic forces, their directions clustered along four orientations: lateral extension, rostral flexion, adduction, and caudal extension. For the entire set of forces (tonic and rhythmic), the same clusters of orientations were found with the addition of a cluster directed as a flexion toward the body. This distribution of force orientations was quite comparable to that obtained with electrical stimulation at the same sites. The map of tonic responses revealed a topographic organization; each type of force orientation was elicited from sites that grouped together in zones at distinct rostrocaudal and depth locations. In the case of rhythmic sequences of force orientations, some were distinctly more common, whereas others were rarely elicited by NMDA. Mapping of the most common rhythms showed that each was elicited from two or three regions of the cord. These regions were close in location to the tonic regions that produced those forces that represented components specific to that rhythm. There was an additional caudal region from which the different rhythms also could be elicited. Taken together, these results support the concept of a modular organization of the motor system in the frog's spinal cord and delineate the topography of these modules. They also suggest that these modules are used by the circuitry underlying rhythmic pattern generation by the spinal cord.

INTRODUCTION

In previous experiments, the output of the frog spinal cord was investigated using electrical microstimulation of the lumbar gray. Before microstimulation, the isometric passive forces recorded at the ankle with the limb placed in different positions define a force field that converges to an equilibrium point of zero forces corresponding to the resting position of the limb. Bizzi et al. (1991) found that after addition of active forces generated by microstimulation, the force field recorded at the ankle remained convergent in most cases, but its equilibrium point shifted to a point close to the periphery of the limb's workspace.

The costs of publication of this article were defrayed in part by the payment of page charges. The article must therefore be hereby marked "*advertisement*" in accordance with 18 U.S.C. Section 1734 solely to indicate this fact.

Furthermore, on systematic exploration of the spinal cord with the technique of electric microstimulation, only a few types of active force fields were found, each specifying an equilibrium point for the limb in space. This observation has led to the concept of modularity of the spinal cord motor system (Bizzi et al. 1991, 1995; Giszter et al. 1993).

With electrical stimulation, it is not clear, even in chronically deafferented preparations what is being stimulated: somas, dendrites, axons, and nerve terminals can all be depolarized by current. In this study, we reexamined the isometric force output of the spinal cord by using a compound that is known to activate only somas and dendrites. To this end, we used *N*-methyl-D-aspartate (NMDA) microiontophoresis with current and duration parameters expected to produce a spread estimated at 150–270 μm radius (see METHODS and RESULTS). Although chemical activation of the spinal cord with excitatory amino acids was accomplished first using glutamate (Cohen and Wallén 1980; Poon 1980), it was soon discovered that NMDA, which is not taken up by the very active glutamate transporters, is a more effective agent (Grillner et al. 1981). In the past, experiments on the spinal cord using NMDA aimed at understanding central pattern generation, and NMDA either bathed the whole spinal cord (Grillner et al. 1988) or was applied topically to the dorsal surface of spinal cord segments (Currie 1994). To our knowledge, this is the first study directed at investigating the spinal cord output using focal intraspinal NMDA iontophoresis. This study provides results relevant both to the modularity of the spinal cord motor system and to the circuitry underlying central pattern generation.

METHODS

Preparation

Thirteen bullfrogs (*Rana catesbeiana*) were anesthetized with 1 ml of tricaine methanesulfonate subcutaneously, supplemented with ice. The cervicomedullary junction was exposed and spinalization carried out by suction at the level of the obex. The back muscles overlying vertebrae 4–6 were removed in preparation for laminectomy. Bipolar electrodes were implanted in 12 hindlimb muscles (rectus internus, adductor magnus, semitendinosus, sartorius, vastus internus, rectus anterior, vastus externus, iliopsoas, biceps femoris, semimembranosus, gastrocnemius, tibialis anterior) to record electromyographic (EMG) activity (to be reported in a separate paper). On the next day, after laminectomy of the fourth, fifth, and sixth vertebrae, the dura was opened with electrocautery and scissors to expose the dorsal surface of the right side of the lumbar spinal cord from above the seventh root to below the tenth root. The pia was opened with fine scissors, and a detailed drawing was made of the exposed spinal cord vasculature and

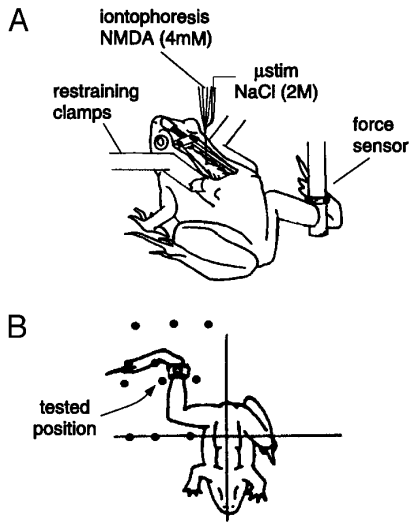

FIG. 1. Apparatus and limb configuration. *A*: apparatus. Spine and pelvis were held clamped by restraints (latter not shown). Micropipette assembly was descended in the spinal cord for electrical stimulation and *N*-methyl-D-aspartate (NMDA) iontophoresis. Mechanical response to stimulation was recorded by the force sensor attached to the limb at the ankle. Limb configuration was constrained by the pelvis restraint and the force sensor. *B*: sketch of the locations in the workspace where recording of isometric forces has led to the recognition of a few types of convergent force fields in prior work with electrical stimulation. In the present study, the ankle was kept in the center of the grid where the orientation of the force vector best distinguishes between the different types of force fields, and points in the direction of the overall flow of the field to its area of convergence. *A* and *B* were modified from Giszter et al. (1993).

dorsal root entry zones, which later served to document the points of entry of the micropipette. Experiments began once all surgery was completed, i.e., 2–3 days after spinalization. Frogs were kept refrigerated between surgical procedures and between experiments (usually 2–3 per frog). All procedures were approved by the animal care committee at our institution.

Micropipette

A three-barrel and a single-barrel pipette were prepared from 1-mm glass capillary tubes using a vertical puller and their tips broken to 2.5 μm. The single barrel pipette was bent 15° under the heat of a coil, first at the shoulder level and then in the reverse direction at the shank level. The lower shanks of the two pipettes then were approximated fully and glued together with cyanoacrylate, the single-barrel tip protruding by 10–15 μm (Crossman et al. 1974). Epoxy glue was added to consolidate the pipette assembly.

The single barrel was filled with 2 M NaCl and connected to an amplifier for microstimulation or recording. The three-barrel pipette was filled with NMDA dissolved in deionized water, 4 mM, pH 8, for iontophoresis (impedance ~100 MΩ), Ringer for current balancing, and 2 M NaCl for stimulation.

Experiment

The spinalized frog was immobilized on a moistened molded stand with body and pelvis clamps. A force sensor attached to the right ankle at the same vertical level as the hip measured the horizontal isometric forces F_x, F_y developed by the hindlimb in response to cord stimulation (Fig. 1*A*). One unit of force was equivalent to ~0.01 N, which corresponded to the resolution of our force transducer. The ankle was at the center of our force field grid designed to sample the leg workspace (Fig. 1*B*). At this location, it is generally possible to distinguish different vector orientations corresponding to the different kinds of force fields resulting from stimulation applied to different parts of the spinal cord (Giszter et al. 1993).

Cord penetrations were made 150–350 μm away from the midline. Depth was measured from the number of microdrive turns from the point of pipette entry as visualized with a microscope. In a single frog, Alcian Blue 3% was pressure-ejected at 11 different sites in the spinal cord, using the single-barrel component of the pipette assembly used in the experiments. On histology, the Alcian Blue spots (found at 6 of the 11 locations) were consistently less deep by 133 ± 104 (SD) μm (correcting for 30% histological shrinkage determined from staining 2 additional superficial sites of known laterality) than our depth estimated from the point of pipette entry. A possible depth overestimation of ~150 μm should be kept in mind when considering the topographic results reported in this paper, which are based on depth estimated with the microdrive.

Electrical stimulation, applied in 100-μm steps, consisted of a 400-ms-long, 40-Hz train of 0.6-ms pulses, with the intensity adjusted to obtain a force response (3–25 μA). Force sampling was at 86 Hz for 2 s, starting 200 ms before the onset of stimulation.

In initial experiments, we iontophoresed NMDA at sites responding to low-intensity electrical stimulation. Later, iontophoresis was attempted first at a depth of 500 μm and then again at depths of 800 and 1,100 μm, especially if there had been no response more superficially. The iontophoretic current was always −100 nA, continued until EMG activity began or for a maximum of 30 s. The forces and EMGs were collected for 40 s beginning with the iontophoresis. Rarely, the 40-s records were begun later, 20–25 s after the onset of a repeated iontophoresis at a site that had responded late to a prior iontophoresis (4 sites). Movements of the contralateral hindlimb were not monitored.

Assessment of drug spread and neural substrate of NMDA action

We estimated the spread of NMDA by computing the radius of tissue exposed to suprathreshold concentrations of NMDA by the average time of onset of forces. We used 15 μM NMDA as a conservative estimate for the threshold concentration: 2.5–100 μM NMDA typically is bath-applied to in vitro whole cord or slice preparations (Alford and Grillner 1990; Barry and O'Donovan 1987; Hochman et al. 1994a,b; Soffe 1996); in dissociated cells, the EC_{50} (half the NMDA concentration that achieves a maximal effect) is 30 μM for the accumulation of cyclic guanosine monophosphate (Garthwaite 1985) and 35 μM for the NMDA receptor current (Patneau and Mayer 1990). The distribution of tissue concentrations of NMDA achieved by iontophoresis was computed using the equation for diffusion from a continuous point source (Carslaw and Jaeger 1959; Curtis et al. 1960; Nicholson et al. 1979)

$$C = \frac{8.25 * 10^{-6} nI}{ZD/_{\lambda^2} r\alpha} \operatorname{erfc} \frac{r * 10^{-4}}{2\sqrt{D/_{\lambda^2} t}} \quad (1)$$

where C is the tissue NMDA concentration (moles/liter) at time t (s) and distance r (μm) from the pipette tip; n the ionic transference number, estimated at 0.3 for NMDA from values for other excitatory amino acids (Stone 1985); I the iontophoretic current (0.1 μA); $Z = 1$, the valency of NMDA; D the diffusion coefficient, estimated from the molecular weight of NMDA at $0.6 * 10^{-5}$ cm^2/s at 25°C (Curtis et al. 1960; Longsworth 1953); $\lambda = 1.6$ and $\alpha = 0.21$, the tortuosity factor and extracellular space fraction respectively (Nicholson and Phillips 1981; Nicholson and Syková 1998); and erfc the complementary error function (Carslaw and Jaeger 1959).

We also estimated the spread of NMDA using another focal

method, slow pressure ejection, where the distribution of tissue concentrations is given by

$$C = \frac{Q}{4\pi D/_{\lambda^2} r\alpha * 10^{-7}} \operatorname{erfc} \frac{r * 10^{-4}}{2\sqrt{D/_{\lambda^2} t}} \quad (2)$$

where Q is the ejected flow rate (moles/s) and the other parameters as in *Eq. 1*.

We also evaluated how much of the NMDA receptor antagonist 2-amino-5-phosphonovaleric acid (APV) had to be applied focally at a previously active site to abolish the response to NMDA. A 60 μM radius APV droplet was pressure-ejected as an ''instantaneous'' point source over 1 s. Its distribution of tissue concentrations is given by (Carslaw and Jaeger 1959; Nicholson 1985)

$$C = \frac{C_f}{2}\left\{\operatorname{erf}\frac{\lambda(r+b)*10^{-4}}{2\sqrt{Dt}} - \operatorname{erf}\frac{\lambda(r-b)*10^{-4}}{2\sqrt{Dt}} - \frac{2}{\lambda r*10^{-4}}\sqrt{\frac{Dt}{\pi}}\left[\exp\left(\frac{-\lambda^2(r-b)^2*10^{-8}}{4Dt}\right) - \exp\left(\frac{-\lambda^2(r+b)^2*10^{-8}}{4Dt}\right)\right]\right\} \quad (3)$$

where C_f is the APV concentration of the ejected droplet, b the ''effective'' radius of the droplet equal to the radius of the ejected droplet divided by $(\alpha)^{1/3}$ ($\alpha = 0.21$, the extracellular space fraction), D the diffusion coefficient of APV estimated at $0.5287 * 10^{-5}$ cm^2/s from its molecular weight, erf the error function, and the other parameters as in *Eq. 1*.

Two concentrations of APV were used: 910 and 520 μM. These were chosen using *Eq. 3* to determine what radius of tissue would be constantly exposed to a $\geq$50 μM APV concentration during the time period that corresponds to the average latency of onset of forces produced by unantagonized NMDA iontophoresis. An APV concentration of 50 μM is considered sufficient to block high NMDA concentrations, such as those achieved near the pipette tip (Davies et al. 1981; Garthwaite 1985). Because APV has a rapid offset (and onset) of action (Mayer et al. 1988), NMDA iontophoresis was begun shortly, i.e., 20 s after the APV application.

To attempt to distinguish between interneurons and dendrites of motoneurons as the two possible substrates of NMDA action, we applied focally tetrodotoxin (TTX) at sites responding to NMDA. TTX blocks conventional Na^+ spike generation. If NMDA acts on local interneurons, their output should be blocked with TTX and the response to NMDA abolished. If NMDA acts on local motoneuron dendrites, their depolarization still should be conducted to the motoneuron somas/initial axons, which are located outside the region of TTX blockade, hence free to spike, and the response to NMDA should not be abolished. A putative amplification mechanism of the NMDA-induced depolarization by other voltage-dependent channels in motoneuron dendrites could potentially be blocked by TTX, thereby decreasing the contribution any direct NMDA-induced motoneuron dendritic activation might have to the response, but this is unlikely to have happened here (see DISCUSSION).

A 100-μm-radius droplet of 20 μM TTX (Turner et al. 1989, 1994) was ejected during 4 s, resulting in an estimated radius of TTX blockade of 300 μm (*Eq. 3*), i.e., the radius with a TTX concentration $>$1 μM (Hochman et al. 1994a,b; Larkum et al. 1996; Schwindt and Crill 1997; Skydsgaard and Hounsgaard 1994). NMDA iontophoresis was repeated 3 min after the application of TTX.

Both APV and TTX applications were done at sites where a prior pressure-ejection of Ringer solution with similar parameters had little or no effect on the response to repeated NMDA iontophoresis. The time between successive NMDA iontophoreses was 11 min. Pressure-ejected drugs were dissolved in Ringer solution and the pH adjusted at 7.3. Pressure-ejection was considered reliable on finding a similar size of the ejected droplet measured in the air with a microscope graticule, before cord penetration and after pullout from the studied site. In these experiments, this occurred with an individual barrel tip size of 1.3 μm for the multibarrel pipette and 3 μm for the single-barrel pipette. It remains possible that a smaller amount was delivered in the tissue than measured in the air. However, this would mean smaller estimates for the NMDA spread and the amount of tissue that needs to be ''blocked'' by APV or TTX to abolish the response to NMDA.

Analysis of forces

For each force record, the initial passive force was subtracted to yield the active force. The force angle was computed from F_x, F_y with the following notation: 0° rostral, $\pm$180° caudal, 90° lateral, $-$90° adduction, and its magnitude was $\sqrt{F_x^2 + F_y^2}$. The time courses of the force angle and magnitude then were plotted.

Because it was observed that the NMDA forces go through steady force angle levels separated by brief transitions, an algorithm was written to automatically detect the onset/offset of the stable forces in each file. The computer algorithm initially detected stable forces as a series of consecutive force samples, where each sample had an angle that differed by no more than 4° from the sample 200 ms earlier and had a magnitude above the noise level of 2 force units. To avoid excessive parsing, stable forces separated by gaps of less than nine samples ($\sim$100 ms) were bridged in the next step of the algorithm into a single stable force. This was deemed acceptable because in force angle plots no transition between clearly different stable force angle levels occurred faster than in nine samples. The automatically detected responses then were verified by visual inspection for stability. A very good agreement was found. For weak responses, corrections were sometimes necessary when they had been excessively parsed by the algorithm. A database thus was constructed listing for each NMDA-responsive site the chemically evoked stable forces fulfilling two criteria: force angle not changing by $>$20°/s and average force magnitude $>$2 (the noise level for individual force samples). For electrical stimulation, the briefer stable responses were determined directly by visual inspection.

We examined the relationship between the response evoked by electrical stimulation and NMDA iontophoresis of a particular site. The absolute difference between the orientations of the first NMDA and electrically evoked forces at each site was calculated and the mean of these differences taken using standard circular statistical methods for directional data (Mardia 1972). We determined, using a randomization test (Fisher 1993) whether this mean difference was significantly smaller than expected if the responses from NMDA and electrical stimulation at a site were unrelated.

The distributions of stable force orientations elicited by NMDA and by electrical stimulation were examined with circular histograms. The number of clusters, or modes, in the distribution of force directions elicited by NMDA was assessed using a method described by Hsu et al. (1986). The essential idea of this method is to find the optimal fit of the observed distribution to a mixture of a given number of modes and then examine the goodness of fit of this mixture to the observed data: if the given mixture is a poor fit to the observed distribution, then it is concluded that there is at least one more mode in the data.

Each mode is described by a probability distribution that gives the probability that a particular data point will be produced by that mode. In the case of circular data considered here, the standard probability model is the von Mises distribution (Fisher 1993; Mardia 1972), described by parameters specifying its mean and concentration (analogous to the mean and variance of the normal distribution). A mixture of von Mises distributions is described by

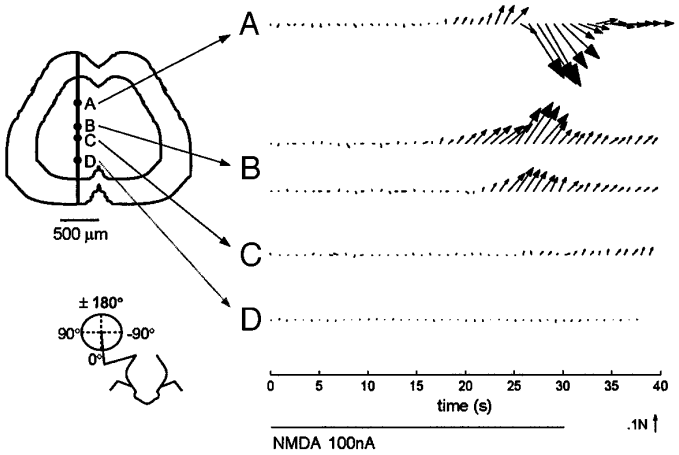

FIG. 2. Effect of repeated NMDA iontophoresis at 1 site and responses at other sites in the same track. Tested depths from the cord dorsum were 673 μm (*A*), 977 μm (*B*), 1,127 μm (*C*), and 1,427 μm (*D*) as shown (*inset*); the order of tested depths was *B, C, D,* and *A.* At *depth B,* the iontophoresis was repeated after an interval of 21 min. For each trial, NMDA iontophoresis started at *time 0* and stopped at 30 s, and every 75th sample of the active isometric force vector is plotted to show its time course (in this and subsequent figures, the 1st 60 ms of force, i.e., resting force, has been subtracted to yield the active force). The force traces are oriented with respect to the frog as shown in the *bottom inset.* All forces are drawn in the same scale (*top right*).

the set of means and concentrations for all of the modes as well as by weighting parameters, which describe how much of the data are produced by each mode.

The optimal fit of a mixture of n von Mises distributions to the observed distribution of data were found using the expectation maximization algorithm (EM), as described by Dempster et al. (1977). Once an optimal fit of a mixture of *n* von Mises distributions to the data was found, the goodness of fit of this mixture was calculated using the U^2 statistic for circular data (Mardia 1972), analogous to the χ^2 statistic for linear data. We assessed the significance of this U^2 statistic using a bootstrap procedure (Hsu et al. 1986). This procedure gave the probability that the data were actually produced by the optimal mixture of *n* modes. A significantly low probability would suggest that the data were likely not to have been produced by the mixture, indicating that there is at least one more mode in the data.

The results obtained from EM also can be used to divide the data into distinct categories: each data point is assigned to the mode that has the highest probability for the data point. A variant of EM, k-means (Hartigan and Wong 1979), also can be used to categorize the data: each data point is assigned to the mode with the nearest mean. K-means will update its mixture model, therefore differently than EM, and the two methods may produce slightly different patterns of results. We therefore compared the results obtained from each method to one another and to our visual inspection of the data.

RESULTS

Focal nature and reproducibility of NMDA iontophoresis

We applied NMDA iontophoretically at 229 sites of 85 different spinal cord penetrations in 13 frogs. These sites were essentially all responsive to electrical stimulation (215/224 tested sites).

Figure 2 illustrates an example of one such penetration. It is clear that the response to NMDA iontophoresis varied at different depths, supporting the focal nature of the iontophoretic technique. At *site A,* a sequence of forces of different orientations was produced. At *site B,* NMDA elicited a force of constant orientation, and this effect was reproducible on repeating iontophoresis at that same site. At *site C,* a much weaker force of similar orientation to that of *site B* was produced. *Site D* remained silent.

Forces were elicited by NMDA at 66/229 (28.8%) of tested sites. The forces began at an average latency of 22.5 ± 8.9 s and were associated with obvious EMG activity in the recorded muscles in all but two cases. The effect of iontophoresis was very reproducible: 13 of the 66 sites were retested and 11 responded again, producing forces and EMGs that were remarkably similar to the first response, although occasionally a force component was removed or added.

No force was elicited by NMDA at 163/229 sites. Of these 163 sites, NMDA actually elicited weak EMG activity at 33 sites, but it was insufficient to produce a force. Repeated iontophoresis at 5 of these 33 sites produced forces at 3 (the onset of recording was delayed with respect to iontophoresis onset in 2 cases), whereas 1 site no longer responded and 1 site still produced weak EMG activity without force. The other 130/163 sites were completely silent with no EMG activity elicited by NMDA. Repeated iontophoresis at 16 of these 130 silent sites still produced no force in 14.

Further evidence demonstrating the presence of active and silent loci was the observation that of 60 penetrations with more than one site tested, 29 had both silent and active sites producing forces. The closest distance between active and silent sites within these tracks was on the average 320 μm and sometimes could be as little as 100 μm.

Assessment of drug spread

Additional evidence for a limited spread of NMDA is found using *Eq. 1* (see METHODS): at 22.5 s after the onset of NMDA iontophoresis, which is the average latency for the onset of the forces, the NMDA tissue concentration is >15 μM only at distances <270 μm from the pipette tip. At two sites responding to NMDA iontophoresis at the average latency of 22.5 s, pressure application of 4 mM NMDA as droplets of 46–62 μm radius ejected during 35–33 s closely reproduced the forces and EMGs elicited by NMDA iontophoresis, albeit at a longer latency of 32 s and to a similar or greater intensity. Using *Eq. 2* (see METHODS), we find that at 32 s, the pressure-ejected NMDA would have reached a tissue concentration >15 μM only at distances <240–285 μm from the pipette tip. At four sites silent to NMDA iontophoresis, pressure-ejection of similar or greater volumes of 4 mM NMDA (55–104 μm radius during 60 s) also produced no effect. Thus the two methods of NMDA application gave similar results both in terms of identifying active and silent sites and in the estimate of spread of NMDA. In our frogs, a sphere of 270-μm radius represents 0.88% of the volume of an average lumbar cord segment (1,000-μm radius and 3,000-μm length).

We could test four sites in one frog with a 60-μm-radius droplet of 910 μM APV (see METHODS). At all four sites, the response to NMDA iontophoresis was abolished completely. In another frog, two active sites were tested with a

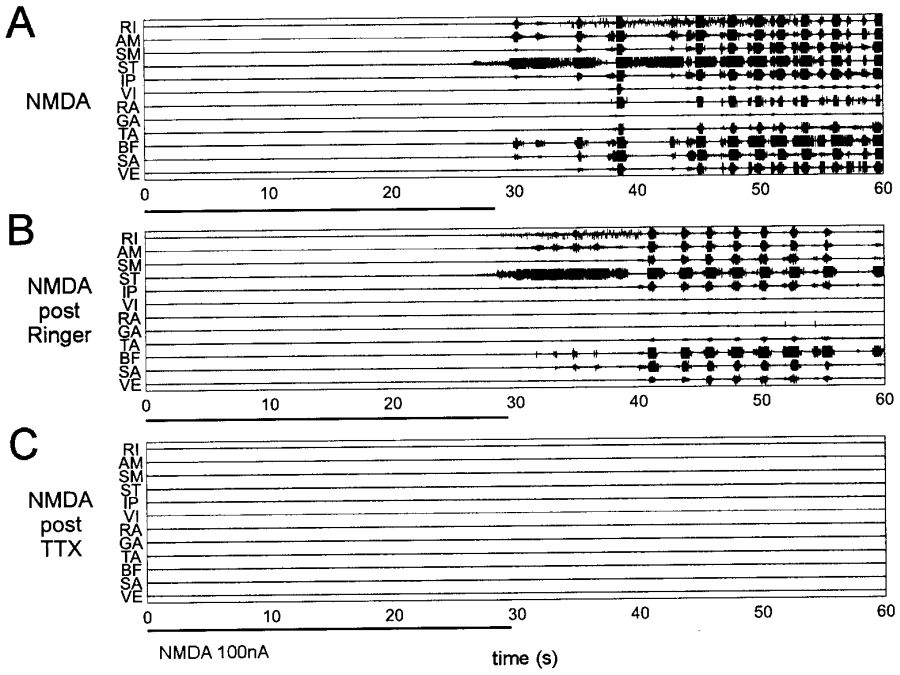

FIG. 3. Effect of a focal application of tetrodotoxin (TTX) at a site responding to NMDA iontophoresis. *A*: electromyographic responses recorded in 12 muscles of the ipsilateral leg in response to NMDA iontophoresis applied for the duration of the horizontal bar. *B*: NMDA iontophoresis repeated 3 min after focal application of a 100-μm-radius droplet of Ringer ejected over 4 s at the iontophoretic site. *C*: NMDA iontophoresis repeated 3 min after focal application of a 100 μm radius droplet of TTX 20 μM ejected over 4 s at the iontophoretic site. Interval between successive NMDA iontophoreses was 11 min. Electromyograms (EMGs) are labeled. RI, rectus internus; AM, adductor magnus; SM, semimembranosus; ST, semitendinosus; IP, iliopsoas; VI, vastus internus; RA, rectus anterior; GA, gastrocnemius; TA, tibialis anterior; BF, biceps femoris; SA, sartorius; VE, vastus externus.

lower concentration of APV (520 μM). The response was again abolished at one site, but APV had no effect at the second site.

At 22.5 s after the onset of NMDA iontophoresis, NMDA concentrations >100 μM would occupy a sphere of 210-μm radius (*Eq. 1*) and would necessitate a 50 μM APV tissue concentration for antagonism (see METHODS). However, *Eq. 3* indicates that with the higher concentration (910 μM) APV droplet, a tissue concentration of APV >50 μM was never achieved beyond a 180-μm radius and that only a radius of 150 μm was constantly exposed to such concentrations during the 22.5-s time period. For the lower concentration (520 μM) APV droplet, which seemed close to threshold to block the effect of NMDA iontophoresis, these figures are 150 and 100 μm, respectively. Finally, similar computations suggest that a tissue concentration >15 μM APV, which would antagonize the lower, more peripheral concentrations of NMDA (Hochman et al. 1994a; Stone 1986), was never achieved beyond a radius of 270–225 μm with the higher and lower concentration APV droplets.

Thus the APV experiments further support a limited direct radius of action of NMDA, which can be estimated at somewhere between 150- and 270-μm radius by the time the active sites began to produce forces.

Neural substrate of NMDA responses

We applied TTX focally at active sites and examined the response to repeated NMDA iontophoresis. The estimated radius of TTX blockade was 300 μm (see METHODS), therefore sparing the motoneuron somas/axons which are located >500 μm away from our deepest iontophoretic sites (see DISCUSSION). At all four sites that we could test in two frogs, the response to NMDA iontophoresis was abolished completely by TTX (with Ringer alone, 2 sites showed no change, 1 potentiation, 1 slight depression). The latter site is shown in Fig. 3. It actually had responded first to a brief iontophoresis of 6 s with a rhythm beginning very early at 4.1 s, but, after a Ringer droplet, had failed to respond again to an equally brief iontophoresis. Because these NMDA applications had been unusually brief, we continued to study this site. Repeated NMDA iontophoresis for 28 s produced a similar rhythm (Fig. 3*A*). After a Ringer droplet, the effect of repeated NMDA iontophoresis, although a bit weaker, was mostly preserved with a qualitatively similar EMG pattern, latency of onset and rhythm frequency (Fig. 3*B*). After the TTX droplet, however, NMDA iontophoresis had absolutely no effect (Fig. 3*C*). By contrast, withdrawal to cutaneous pinch of the ipsilateral foot remained easy to elicit and entirely normal, as judged by EMGs.

The abolition of the responses to NMDA by a focal application of TTX, which blocked the local interneurons but did not reach the motoneuronal somas/axons, supports the idea that the substrate of our NMDA effects is interneuronal.

General features of NMDA responses

In this paper, we report on 69 active sites (66 of which produced forces in response to a 1st NMDA iontophoresis and 3 of which elicited only EMGs to a first iontophoresis but produced forces to repeated iontophoresis).

Figure 4 shows examples from two sites of the two main types of responses to NMDA: a tonic response where the force angle remained steady throughout the recording (Fig. 4*A*) and a rhythmical response where the force angle went through a succession of stable plateaus separated by rapid transitions (Fig. 4*B*). For these rhythms, which represented the more common NMDA effect, the record was parsed to obtain the angle values of the successive stable forces (see METHODS). For example, the rhythmic record illustrated in Fig. 4*B* was parsed into 12 stable forces. A total of 388 NMDA-elicited stable forces were recorded at the 69 sites (one 40-s force record per site).

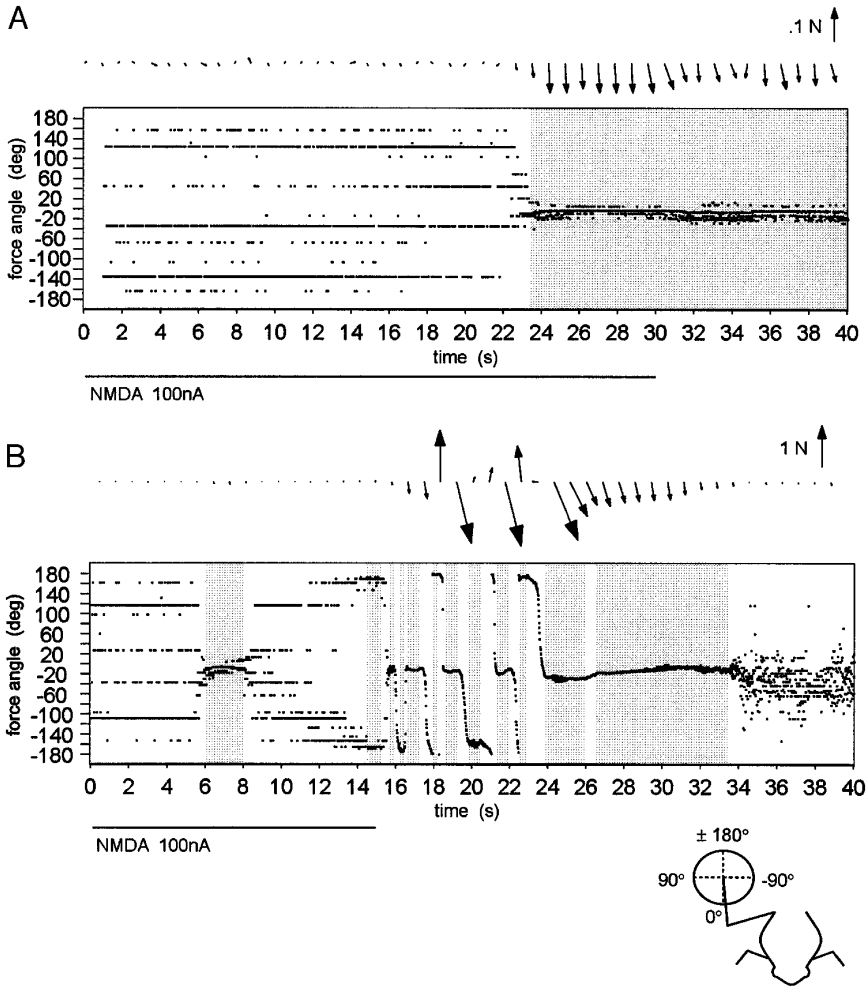

FIG. 4. Tonic and rhythmic effects of NMDA. In each example, NMDA iontophoresis was applied for the duration of the horizontal bar, and every 75th sample of the active force vector is shown (*top*) with its magnitude scaled as indicated. Angle of that force vector was plotted over time, with the convention for the force orientation as shown (*inset*). In each record, the shaded regions identify the stable forces. *A*: example of a tonic effect. *B*: example of a rhythmic effect. *A* and *B* are from 2 different frogs.

Comparison between NMDA and electrical stimulation

We compared the orientations of the chemically and electrically evoked forces at each of the 69 NMDA-responsive sites. This was not straightforward because NMDA commonly produced a sequence of forces as did electrical stimulation although less frequently. Moreover electrical stimulation often was tested at several intensities, sometimes with a change in the orientation of the force. We therefore compared in the force sequences the first NMDA-evoked force and the first electrically evoked force, selecting for the latter the one closest in amplitude to the chemically evoked force. The distribution of the absolute difference in orientation between these two responses at the same site is shown in Fig. 5. Although there is a wide variation in angular differences between the two responses, with large differences not being uncommon, this difference was small at the majority of sites. The mean difference was 49°, which was significantly less than the one expected (68°) if there was no relationship between the two responses (randomization test, $P < 0.001$). Thus there was a relationship, though not very strong, between the force orientation elicited by NMDA and by electrical stimulation at the same site.

Clusters of force orientations

Next we examined how the force orientations elicited by NMDA and by electrical stimulation were distributed for the entire set of 69 NMDA-responsive sites. The distribution for the NMDA-elicited stable forces, obtained by parsing the records as indicated in Fig. 4, is shown in the circular histogram of Fig. 6. It is clear that some force orientations happened at greater frequency than others. Specifically, a careful

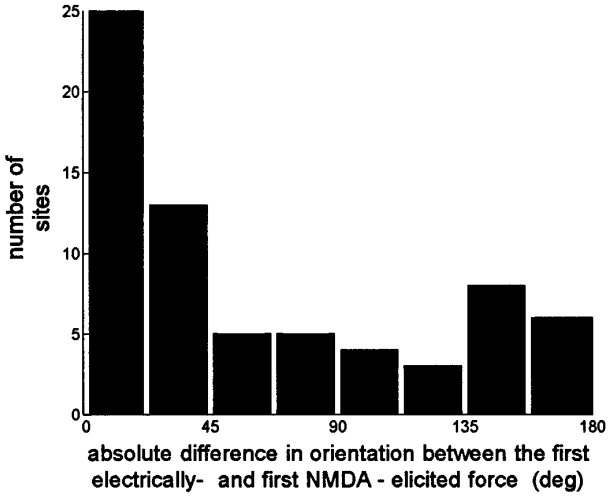

FIG. 5. Distribution of the absolute difference in orientation between the 1st electrically evoked force and the 1st NMDA-evoked force at each NMDA-responsive site ($n = 69$).

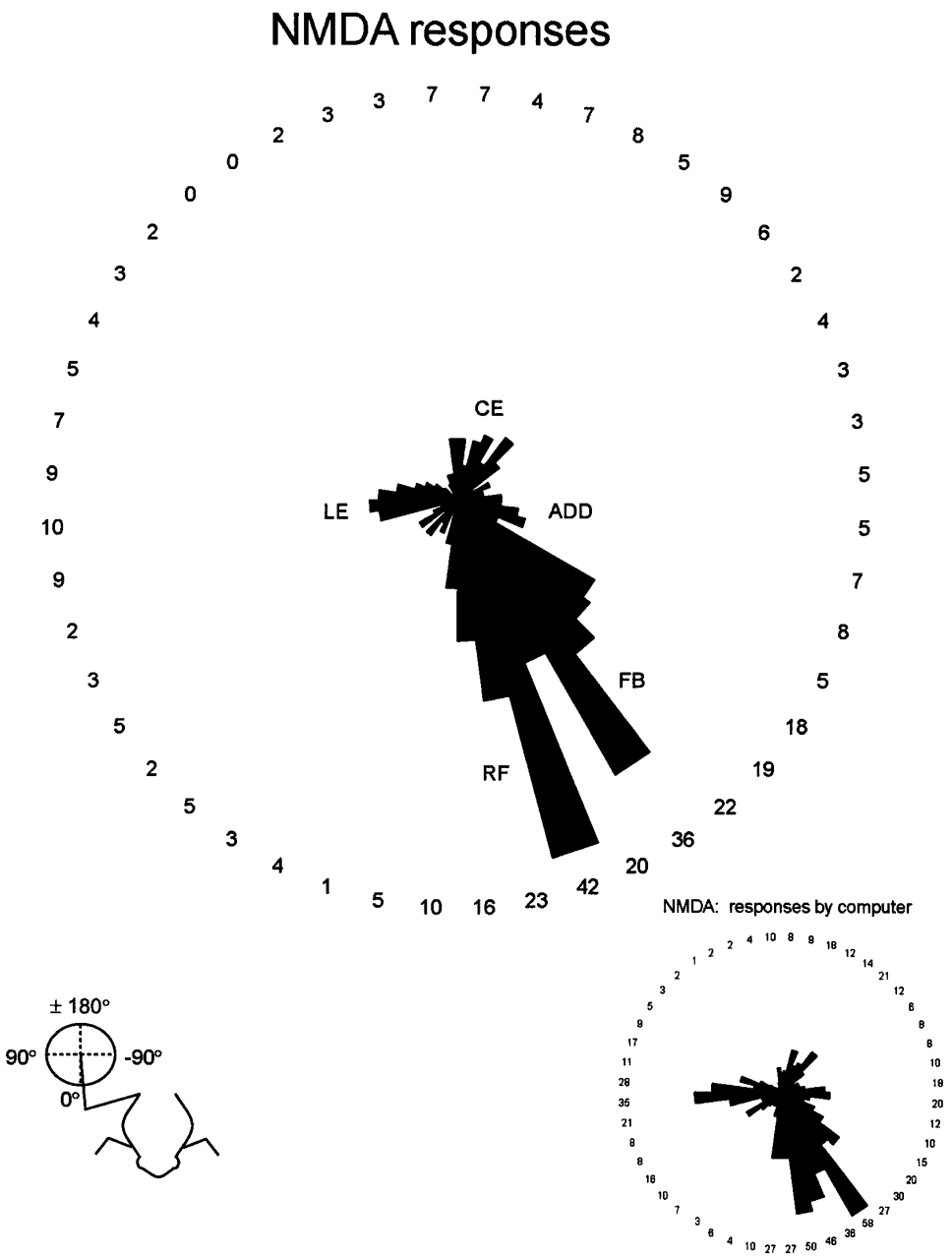

FIG. 6. Orientations of the NMDA-elicited forces ($n = 388$) obtained in 13 frogs from 69 spinal cord sites, that responded to NMDA. Circular histogram of 7.5° binwidth, oriented with respect to the frog as shown (*bottom left inset*). Number of responses in each bin is displayed. Clusters of force orientations are labeled. LE, lateral extension; RF, rostral flexion; FB, flexion to body; ADD, adduction; CE, caudal extension. A similar histogram was obtained when plotting directly the responses automatically detected by the computer algorithm without any correction (*bottom right inset*).

visual inspection of Fig. 6 suggests that the force orientations clustered in five preferred directions. These clusters are labeled as lateral extension (LE), rostral flexion (RF), flexion to body (FB), adduction (ADD), and caudal extension (CE), a terminology based on the direction the ankle would move if it were free to do so (Giszter et al. 1993). Figure 7 shows the stable force angles obtained with electrical stimulation at the same 69 sites. It can be seen that the two distributions of force orientations, one from NMDA application, the other from electrical stimulation, are similar in their main features. In particular, similar clusters of preferred force orientations appear to be present in Figs. 6 and 7.

To verify this visual impression of several clusters, we analyzed further the distribution of force orientations elicited by NMDA iontophoresis, using a method aimed at estimating the number of modes within this distribution (Hsu et al. 1986) (see METHODS). There was strong evidence to suggest the existence of at least five modes in the distribution ($P < 0.01$, 0.05, 0.05 for $n = 2$, 3, and 4 modes, respectively). A test for the existence of six modes failed to reach significance, although the probability value approached a trend ($P = 0.12$). This analysis therefore allows us to conclude that there are at least five modes of force orientation within the responses produced by NMDA.

The identification of these modes was done using both the EM and the k-means algorithms (Dempster et al. 1977; Hartigan and Wong 1979) (see METHODS). For five modes, the two methods produced different patterns of classification. K-means divided the data into five clusters corresponding to the LE, CE, ADD, FB, and RF clusters (Fig. 8*B*) identified from our own visual inspection as described above. EM, on the other hand (Fig. 8*A*, *left*), appeared to identify the

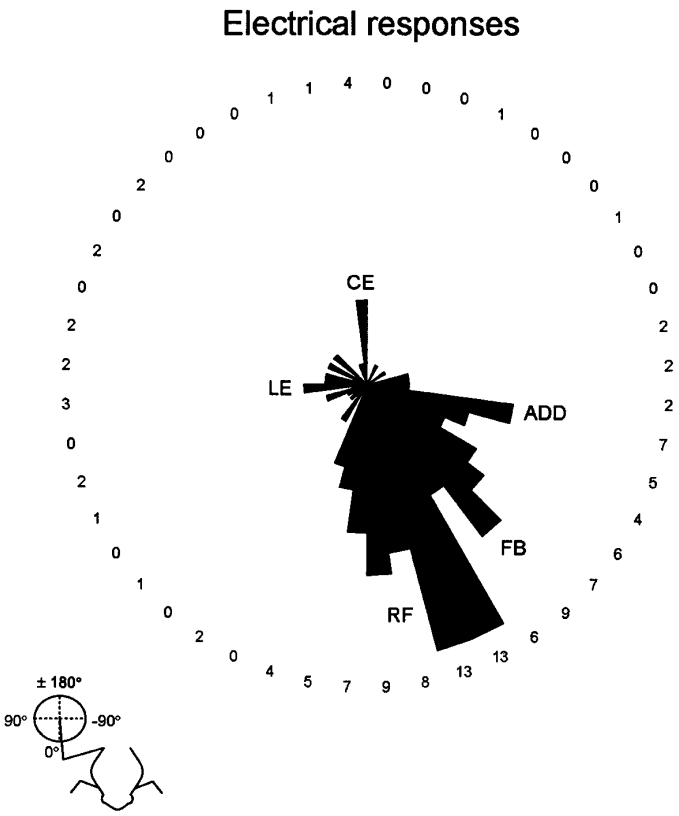

FIG. 7. Orientations of the forces elicited by electrical stimulation (n = 134) at the 69 NMDA-responsive sites of Fig. 6. Circular histogram of 7.5° binwidth. Number of responses in each bin is displayed. Clusters of force orientations are labeled as in Fig. 6.

LE, CE, and ADD clusters but did not achieve separation between RF and FB and found an additional cluster centered at ~45°. When the number of clusters was increased to six, however, both methods produced a very similar classification. Both EM (Fig. 8*A*, *right*) and k-means (data not shown) found essentially the same six clusters: the five main ones identified by visual inspection plus the cluster near 45°. The exact divisions between the six modes were not identical, but the main classes were the same. Given that the statistical analysis described earlier allowed us to conclude the presence of only five modes in the data and that *k*-means identified the same five modes we found from visual inspection of the data in Fig. 6 and from other analyses (see for instance Figs. 7 and 15), in the rest of this section, we present results based on a classification of the data according to the divisions identified by k-means with five modes. We also have analyzed the results obtained using the divisions identified by EM with five or six modes as well by k-means with six modes, and although the details are slightly altered in each case, the basic pattern of results we report here are the same.

In summary, analysis of the NMDA data by the three methods, i.e., visual inspection, clustering by the EM algorithm, and clustering by k-means, suggests the existence of five main clusters of force orientations (LE, RF, FB, ADD, CE). Comparison with electrical stimulation supports this clustering. The NMDA force data thus were divided into the five categories shown in Fig. 8*B*. Using these divisions, we next examined the organization of the responses evoked by iontophoresis of NMDA.

Comparison of tonic and rhythmic forces

An important finding was that only a subset of the NMDA-responsive sites produced a simple tonic response. Tonic forces were elicited from 18 sites in 10 frogs (an example was shown in Fig. 4*A*). Their orientations are plotted in Fig. 9. They included LE, RF, ADD, and CE, but it is noteworthy that no tonic FB was obtained.

Thus the entire set of NMDA forces (Fig. 6), which mostly came from rhythmic sites, consisted of the *same* four orientations as the tonic forces (Fig. 9) + FB. This finding by itself is suggestive of some sort of spinal cord organization whereby the more complex rhythmic responses would be built from the simpler ones. To evaluate this further, we examined the topography of the sites that produced tonic forces and compared it with that of the rhythmic sites.

Topography of NMDA responses

Figure 10 shows for each force component the relative frequency with which it was seen among the different rhythmic forces elicited from each spinal cord segment. A one-way analysis of variance performed on that data showed a highly significant relationship between rhythmic force component orientation and the rostrocaudal location of the rhythmic site [$F(4,347) = 12.65$, $P < 0.001$]. In particular, a clear difference is seen between LE and CE in Fig. 10, and this was confirmed by a post hoc *t*-test [Scheffé $F(4,347) = 9.46$, $P < 0.001$]. Segments 9,10 were the most likely to produce a LE rhythmic component, whereas segments 7,8 were the most likely to produce a CE rhythmic component. For ADD, FB, and RF, the distributions of relative frequency of occurrence along the cord in Fig. 10 were intermediate between those for LE and CE, i.e., they were less caudally biased than for LE and less rostrally biased than for CE; however, these distributions did not show clear peaks, but were rather widespread.

The sites where NMDA elicited tonic responses are shown in Fig. 11*A*, and their rostrocaudal and depth locations did define a coarse topography. CE and ADD were obtained more superficially (depths of 860 ± 189 μm and 881 ± 121 μm, respectively) than RF and LE (depths of 1,098 ± 171 μm and 1,324 ± 142 μm, respectively). In rostrocaudal order, NMDA elicited CE (lower segment 7 to midsegment 8, except for 1 instance), RF (segment 8), ADD (lower segment 8), LE (midsegment 9 to midsegment 10). It can be seen that the tonic LE and CE zones, which are the most distinctly apart in Fig. 11*A*, are located in those same cord segments where the highest fractions of rhythmic forces were observed for these force components (Fig. 10).

We examined whether the strongest rhythmic forces (mag >40) have a topography related to that of the tonic zones. Figure 11*B* shows that strong rhythmic LE and CE were again obtained from sites close to the tonic LE and CE zones. Furthermore strong rhythmic ADD were elicited from sites not far from the tonic ADD zone. With respect to strong rhythmic RF, some were elicited from sites close to the tonic RF zone, but others were elicited from sites close to the tonic LE zone.

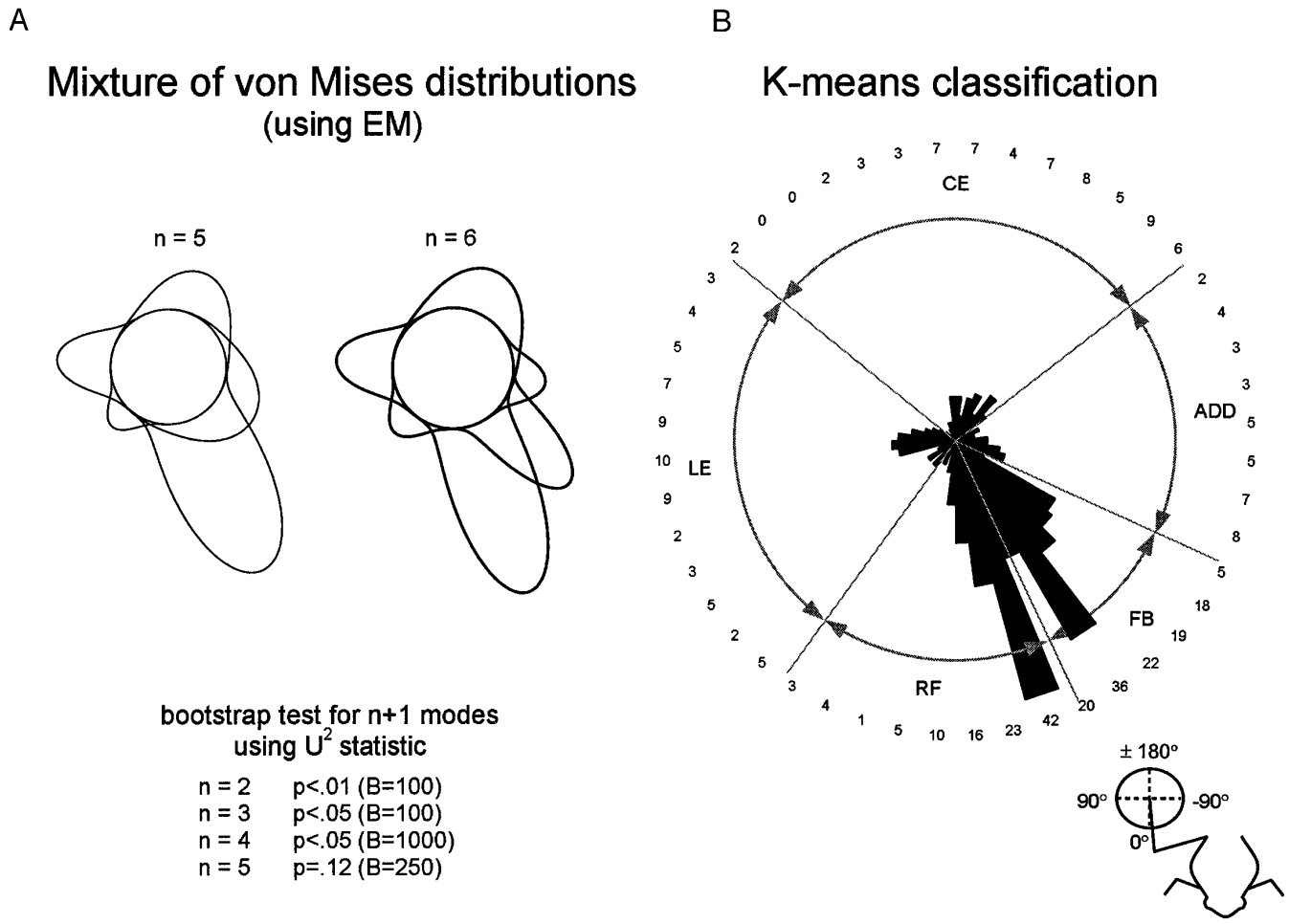

FIG. 8. Clustering analyses. *A*: distribution of stable force orientations elicited by NMDA (reproduced in *B*) was modeled as a mixture of 5 or 6 von Mises probability distributions, which are shown plotted on a circle, with the usual orientation convention relative to the frog. *P* values *below* evaluate the null hypothesis that the NMDA directional data could have been generated by a mixture of a smaller number (≤ 5) probability distributions. *B* is the number of repetitions of the bootstrap procedure. *B*: partitioning of the NMDA-elicited forces into 5 clusters by the k-means algorithm.

This may not be surprising because by definition rhythmic sites produce at least two different kinds of force orientations, and therefore there could be more than one candidate tonic zone close to which they might be located. Indeed of the five rhythmic sites close to the tonic LE zone that produced a strong RF in Fig. 11*B*, four also produced a LE.

This last observation raises the more general problem of connectivity. Given that a topographic relationship appears to exist between the rhythms and the tonic zones according to force orientation, how would the latter be used in the construction of a rhythm with several force components of different orientations?

A clue to connectivity would be finding that some rhythmic combinations of forces occurred more commonly than others. The topography of such rhythms could then be compared with that of the tonic responses. Figure 12 lists the rhythmic responses elicited by NMDA at 44 spinal cord sites from 13 frogs. It is clear from Fig. 12 that some rhythms were more frequent than others, whereas others were not obtained at all. The most frequently seen rhythms were RF,FB; LE,RF,FB; ADD,CE,FB. Examples where NMDA elicited many cycles are shown for each of these rhythms in Fig. 13. The distinction between the RF,FB and LE,RF,FB rhythms was evident early in records because nearly all cases of the LE, RF,FB rhythm started with LE or with RF followed by LE. The occurrence of rhythms alternating between neighboring clusters of Fig. 6 (e.g., RF and FB in Fig. 13*A*) lends further support to the distinction between these clusters.

We can now compare the topography of the sites from which the tonic responses and the three most common NMDA rhythms were obtained.

Figure 14*A* reproduces the map of the tonic responses. Figure 14*B* shows the sites from which a RF,FB rhythm was obtained. In this rhythm, the greatest percentage of cycle time was spent in RF. It was elicited from a zone in segment 8, which had a similar extent to the tonic RF area, and from a caudal zone in segment 10.

Figure 14*C* shows the sites from which a LE,RF,FB rhythm was obtained. RF was only a short phase in contrast to the previous rhythm, and the greatest percentage of cycle time was spent in LE. This rhythm was elicited from a zone in segment 9 located superficially to the tonic LE area and from a caudal zone in segment 10. Sites eliciting the LE,RF and LE,FB subsets of that rhythm again had LE as the longer

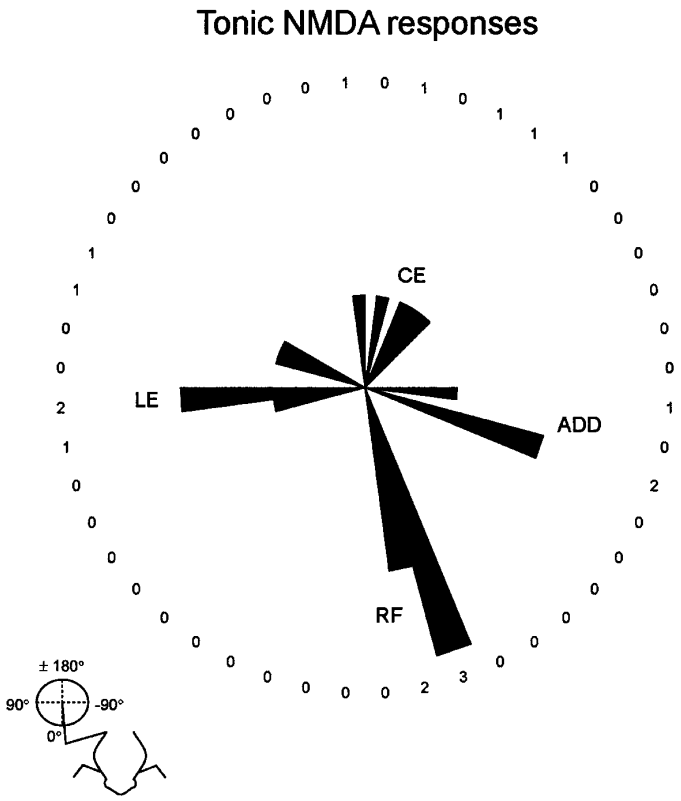

FIG. 9. Orientations of the tonic force responses elicited by NMDA at 18 of the 69 sites of Fig. 6. Circular histogram of 7.5° binwidth. Abbreviations for labels as in Fig. 6. No tonic FB was obtained.

phase and had a similar topography. They have been added to Fig. 14*C* with different symbols.

Figure 14*D* shows the sites from which an ADD,CE,FB rhythm was elicited. They occupied three zones: one in segment 7, which overlapped the tonic CE area, one in midsegment 8, and a caudal zone in segment 10. Sites eliciting the subsets ADD,CE; ADD,FB; and CE,FB of that rhythm had a similar topography and have been added to Fig. 14*D* with different symbols. The zone in segment 8 now can be seen to extend to upper segment 9 and to include the tonic ADD area.

Overall, Fig. 14, *B–D,* suggests that each of the most frequent rhythms could be elicited from two or three regions of the cord. These consisted of regions similar to or close in location to the tonic regions capable of producing those forces that represented components specific to that rhythm, as well as an additional caudal region in segment 10 from which any of these rhythms could be elicited.

The close relationship between regions evoking tonic forces and rhythms made up of the corresponding force components also can be appreciated from the observation that in those few cases where repeated iontophoresis at the same site produced a partly different response, the change was from a tonic RF to a RF,FB sequence (1 site in the tonic RF zone), and from an ADD,CE,FB rhythm to a FB,ADD sequence (1 site close to the tonic ADD zone).

DISCUSSION

The most important result of this paper is that the spinal cord produces a limited number of discrete motor outputs, identified as five preferential directions of the isometric force vector recorded at the ankle in a single limb position. These are: lateral extension, rostral flexion, flexion to body, adduction, and caudal extension (Fig. 6). This confirms the earlier report of a small number of convergent force field types with equilibrium points in the lateral, rostral, flexed to body, adducted, and caudal locations of the workspace produced by electrical stimulation of the frog spinal cord (Bizzi et al. 1991).

Here, however, only a fraction of the sites responding to electrical stimulation responded to NMDA. Assuming a limited spread of NMDA, these sites would correspond to the locations of the somas and dendrites of neurons, which, through their connectivity, produce convergent force fields. The focality of our method of NMDA application in fact seems critical because it has not been possible to induce rhythmic oscillations with bath-application of NMDA to the adult frog spinal cord unless it had been preincubated with strychnine to remove inhibition (Rioult-Pedotti 1997).

The limited spread of NMDA in our study is supported by the finding that the great majority of tested sites did not respond to NMDA iontophoresis. In addition, our observation that silent and active sites could sometimes be separated by as little as 100 μm further supports this notion. Computation of the distribution of tissue concentrations of NMDA also indicated that concentrations of NMDA >15 μM (a conservative estimate for the threshold concentration) were limited to a radius of 270 μm by the average time of onset of force production (this radius fell to 150 μm for the sites responding at the shortest latencies). A similar result was obtained for doses of pressure-ejected NMDA that closely mimicked the effect of iontophoresis. Finally, our experiments with the focal application of APV suggest that expo-

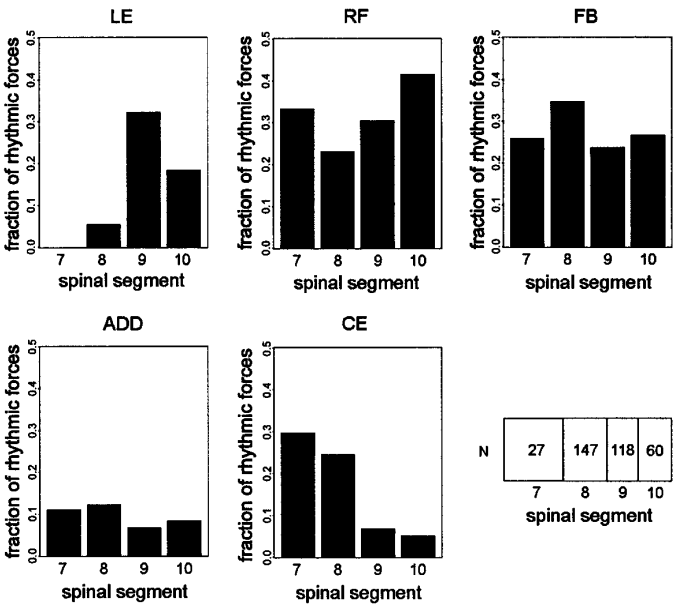

FIG. 10. Relative frequencies with which each force component occurred among the rhythmic forces elicited from the different spinal cord segments. Numbers of NMDA-elicited rhythmic forces from segments 7 to 10 were $n = 27$, 147, 118, and 60 as indicated in the spinal cord diagram. These rhythmic forces were generated from $n = 5$, 16, 9, and 12 rhythmic sites located in segments 7–10, respectively. Of the 44 rhythms in Fig. 12, 2 are missing here (1 from segment 11 and 1 of unknown topography).

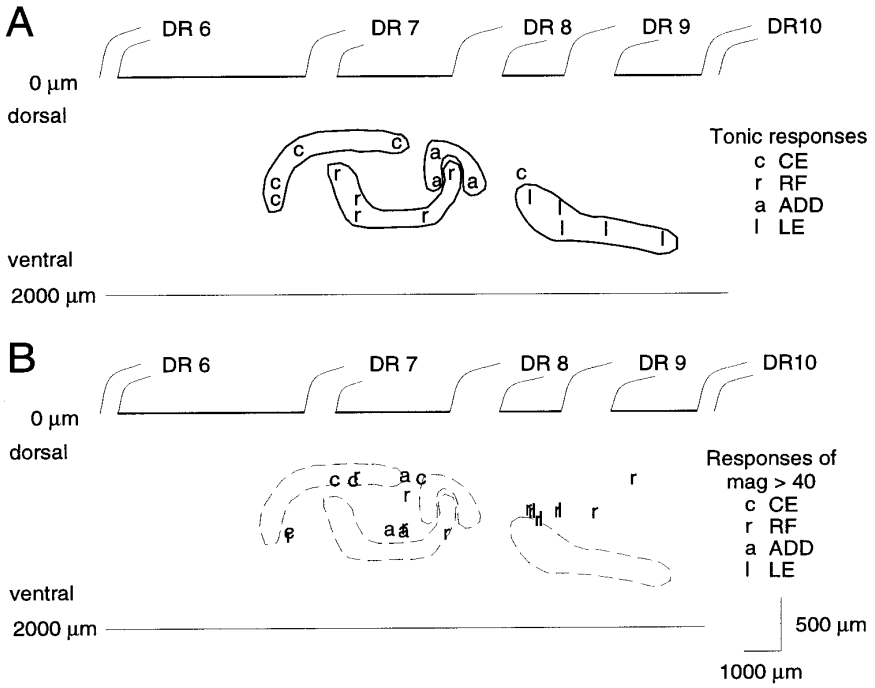

FIG. 11. Topography of the sites producing tonic forces and of the sites producing strong rhythmic forces. *A*: topography of the 18 spinal cord sites where NMDA elicited a tonic response (10 frogs). Depth is vertical with the dorsal and ventral surfaces at depths of 0 and 2,000 μm, respectively. Rostrocaudally, dorsal roots DR6–DR10 delimit the positions of segments 7–10. Note the different scales for the dorsoventral and rostrocaudal axes. All sites were located 150–350 μm from the midline. Four different kinds of tonic responses are indicated by the different letter symbols. Outlines have been drawn to suggest how these tonic responses define a coarse topography. c, caudal extension; *r*, rostral flexion; a, adduction; l, lateral extension. *B*: topography of NMDA-elicited rhythmic forces of the same orientations than the tonic forces and of magnitude >40, in relation to the zones eliciting tonic responses. Force labels as in Fig. 11*A*. Superimposed labels indicate that >1 kind of force orientation with magnitude >40 was obtained at the site. For example, there are 3 sites below DR8 that gave both r and l responses of magnitude >40. As an aid to the reader, the suggested topography of the tonic zones has been reproduced in dotted outlines in Fig. 11*B* to facilitate comparison with the topography of the strong rhythmic forces.

sure of an estimated radius of 150–180 μm, and sometimes as little as 100–150 μm, to a ≥50 μM concentration of APV, adequate to antagonize the >100 μM concentrations of NMDA produced by iontophoresis at such distances, was sufficient to abolish the response to NMDA.

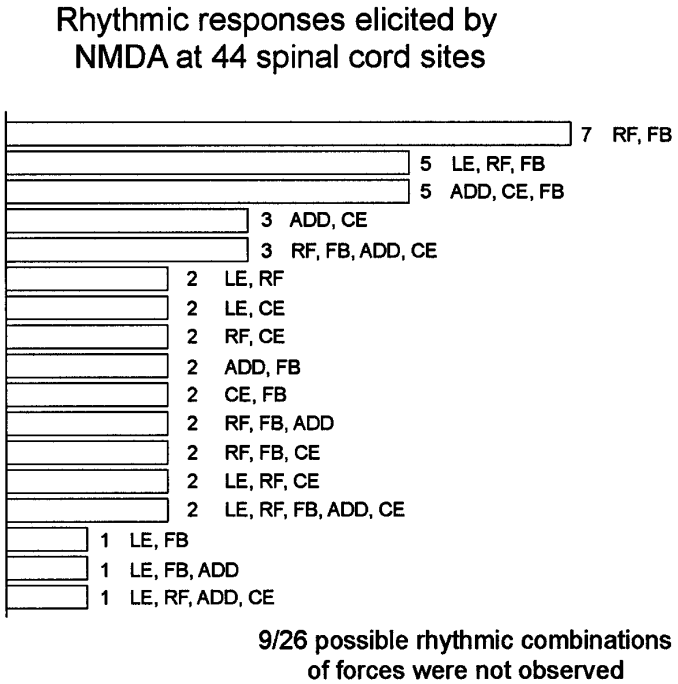

FIG. 12. Rhythmic responses elicited by NMDA at 44 spinal cord sites (13 frogs). Number of sites at which each rhythm with the indicated force components was obtained is indicated. Besides these 44 rhythmic sites and the 18 tonic sites, the other 7 NMDA-responsive sites included 4 sites with single phasic responses and 3 sites that did not fit any category essentially because they produced a force changing sufficiently in angle not to qualify as a tonic response, yet remaining within the same cluster of force orientation.

Thus all these observations indicate that a limited physical spread of NMDA had occurred by the time that activated circuitry, through its connectivity, had begun to produce a force output.

It is not surprising that we found mismatches between the effects of electrical and chemical microstimulation at the same site. Considering that the elements most excitable to electrical stimulation are somas and axons, whereas the most responsive elements to NMDA are dendrites and somas, differences should be expected between the two methods of stimulation. However, the central result remains that the two methods give the same overall picture for the discrete outputs of the spinal cord (Figs. 6 and 7). This discreteness is not the result of biomechanical limitations because one can easily obtain, by directly stimulating the appropriate pair of muscles or by stimulating the vestibular system, strong forces in orientations not produced by spinal cord stimulation (D'Avella and Bizzi 1998; unpublished observations).

The discrete set of force orientations is likely to reflect a fundamental feature in the organization of the spinal cord. This suggestion is strengthened by the finding that tonic sites, which produced a single kind of force from that set, were not at all haphazardly distributed in the spinal cord but clustered in specific regions of the cord according to the force orientation (Fig. 11*A*). Taken together, the discreteness of force orientations emitted by the spinal cord and their organized mapping on the spinal cord, first noted with electrical stimulation (Bizzi et al. 1991) and now confirmed with NMDA, support the concept of a modular organization of the spinal cord motor circuitry (Bizzi et al. 1995).

What is the neural substrate of these modules? The preceding argumentation about spread makes it very unlikely that NMDA directly reached motoneuron somas, which are approximately located at a depth of 1,500 μm and laterality of 700 μm (i.e., >500 μm away from our deepest iontophoretic

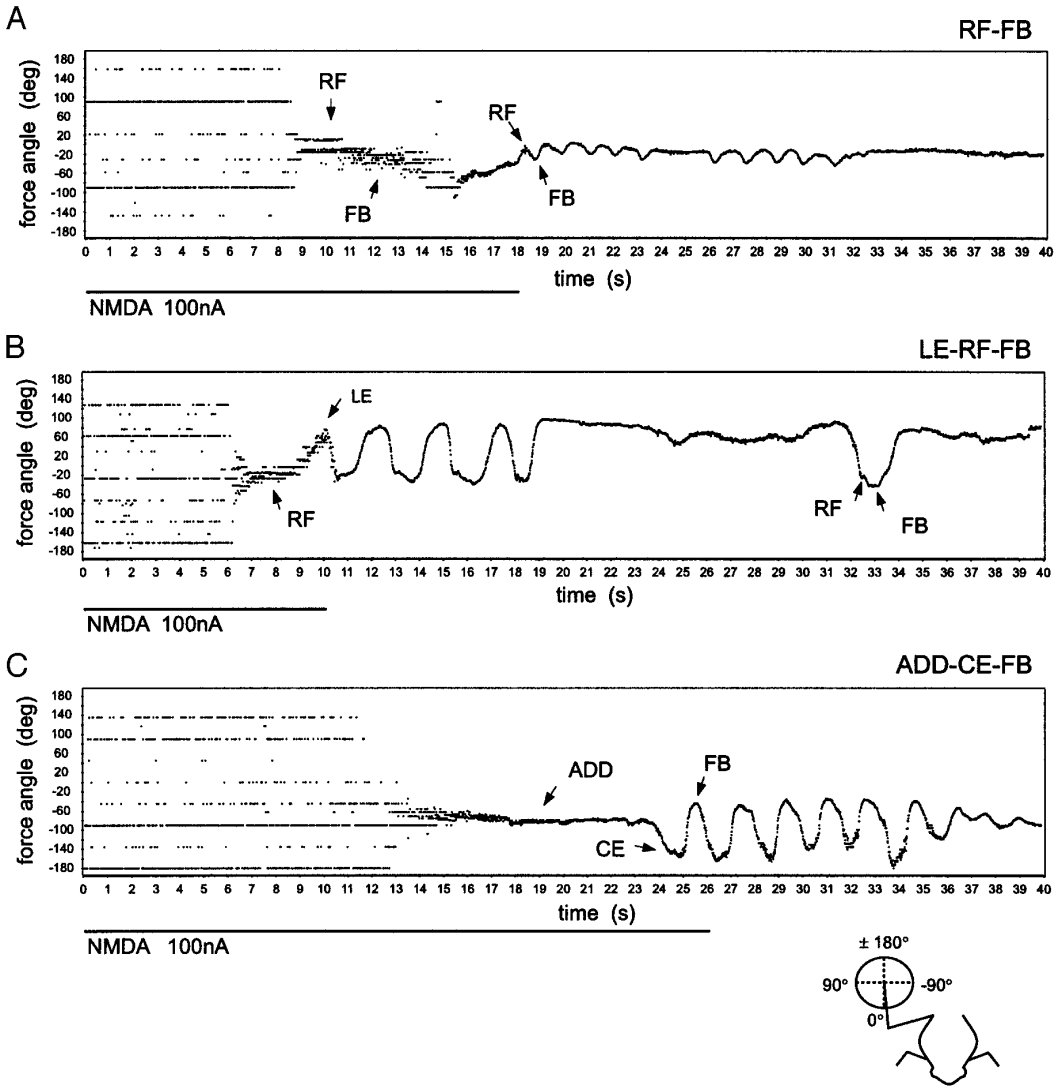

FIG. 13. Well-developed rhythms of the 3 most common combinations of forces elicited by NMDA iontophoresis in the frog's spinal cord (see Fig. 12). *A*: RF,FB rhythm. *B*: LE,RF,FB rhythm. *C*: ADD,CE,FB rhythm. Component forces of these rhythms are identified in the figures (→). *A* and *B* are rhythms from the same frog as the rhythm of Fig. 4*B*. *C* is a rhythm from the same frog as the tonic response of Fig. 4*A*.

sites); but motoneurons have an extensive dendritic arbor that reaches the interneuronal regions where NMDA was administered (Székely 1976), and there is some evidence, mostly indirect, that motoneurons have dendritic NMDA receptors (Durand 1991; Moore et al. 1995; Petralia et al. 1994; Skydsgaard and Hounsgaard 1994; see, however, Robinson and Ellenberger 1997).

At active sites, the exposure of an estimated radius of 300 μm to a blocking concentration of TTX (>1 μM) was sufficient to abolish the response to NMDA in all cases. This focally applied TTX should have spared the motoneuronal somas and axons, and even their proximal dendrites (3 of our 4 TTX application sites were at depths of 820–850 μm, 200–400 μm from the midline, i.e., the periphery of the region of TTX blockade was ~475 μm away from the closest motoneuron somas). TTX will have reached the local distal motoneuron dendrites where it possibly could have influenced direct NMDA-induced depolarization of motoneurons (but see following text). And certainly TTX should have abolished spiking of those interneurons activated by NMDA, which had their somas/initial axons still located within the radius of spread of TTX.

The abolition of the response to NMDA by TTX is therefore entirely consistent with the locus of action being interneuronal. One concern is whether any direct action of NMDA on local distal motoneuron dendrites could have been made less effective by the focal application of TTX. In pyramidal cells of the mammalian hippocampus and neocortex, mechanisms exist to amplify distal dendritic excitatory postsynaptic potentials (EPSPs) on their way to the soma (Schwindt and Crill 1995, 1997). However, the channels responsible for this amplification appear to be located on the axosomatic membrane or the proximal dendrites (Seamans et al. 1997; Stuart and Sakmann 1995) rather than on the distal dendrites themselves, hence outside the level at which motoneurons were exposed to our focal applications of TTX. Moreover in motoneurons there is indirect evidence that amplification of dendritic EPSPs may rely on TTX-

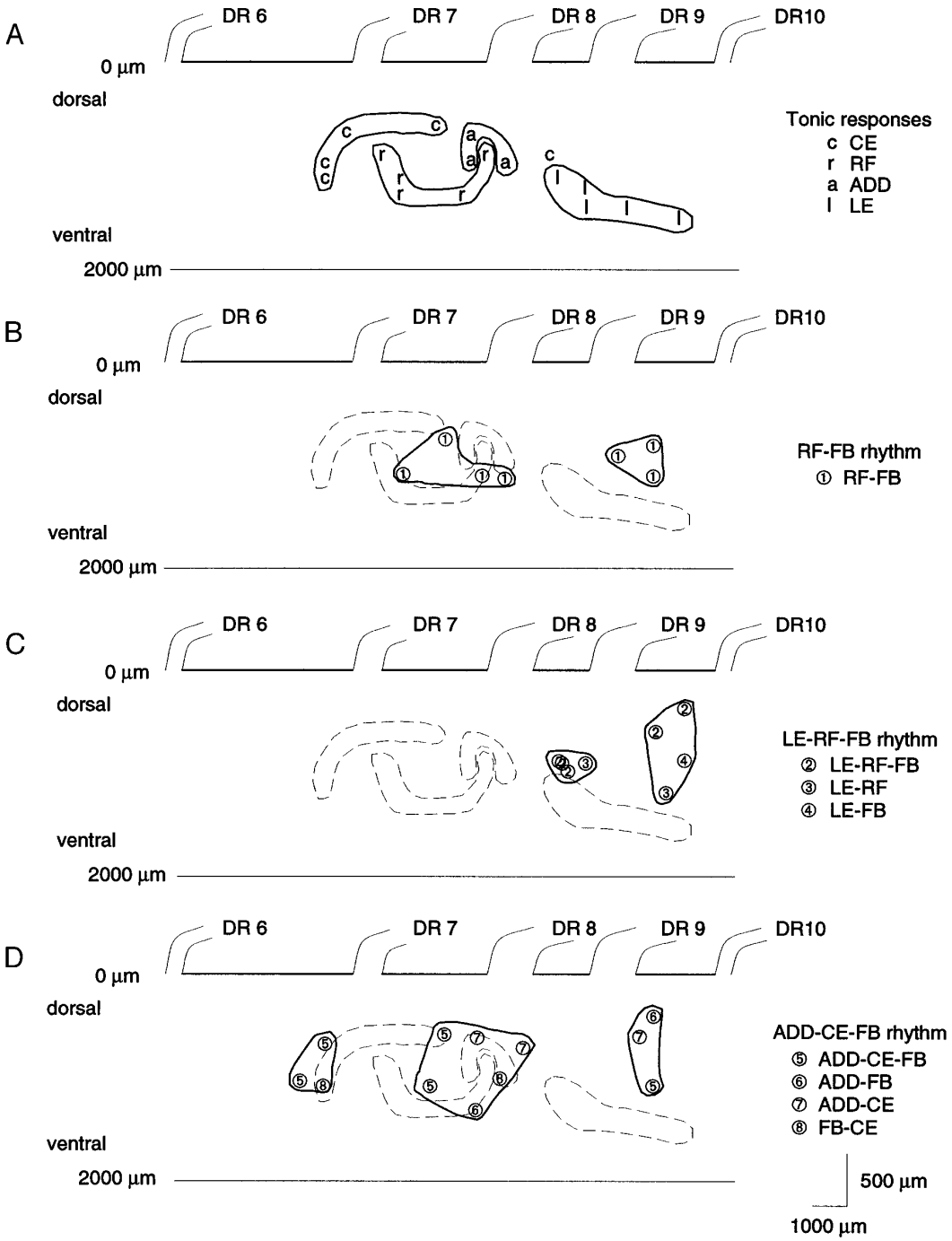

FIG. 14. Topography of the spinal cord sites where NMDA elicited a tonic response or 1 of the 3 most common rhythms. *A*: topography of the 4 different kinds of tonic responses as in Fig. 11*A*. *B*: sites eliciting the RF,FB rhythm. *C*: sites eliciting the LE,RF,FB rhythm and the LE,RF and LE,FB subsets. *D*: sites eliciting the ADD,CE,FB rhythm and the indicated subsets.

resistant Ca^{2+} mechanisms (Hounsgaard and Kiehn 1993; Lee and Heckman 1996; Svirskis and Hounsgaard 1997). In addition, two investigations suggest that blockade of putative TTX-sensitive Na^+ channels in motoneuron dendrites at the site of NMDA iontophoresis does not account for the abolishing effect of focal TTX: *1*) large membrane voltage oscillations can be induced in motoneurons of rat spinal cord slices by bath-application of NMDA in the presence of bath-applied TTX (Hochman et al. 1994a); and *2*) in turtle spinal cord slices, NMDA focally applied in the white matter to distal dendrites of motoneurons produced a depolarization but no spikes recorded at the motoneuron soma level even with more vigorous iontophoresis than ours. However, NMDA iontophoresis amplified the response caused by glutamate applied to the same dendrite into a larger depolarization or even to spikes or oscillatory regenerative events, and this amplification mechanism was TTX resistant (Skydsgaard and Hounsgaard 1994).

In summary, in our experiments with focally applied TTX, NMDA-activated TTX-resistant mechanisms were free to

take place in distal motoneuron dendrites (and presumably also interneuron dendrites); moreover, unlike the situation for the local interneurons, the remotely located motoneuron somas/axons were free to spike, yet the response to NMDA was completely abolished (Fig. 3). The most likely interpretation is that local interneuronal activation, through its connectivity, was responsible for the effect of NMDA in our experiments.

Although EMGs will be reported in a later paper, they also provide evidence that the circuitry activated by NMDA was functional. This evidence consists in the marked similarity between the EMGs elicited by cutaneous stimulation and NMDA spinal microstimulation (unpublished results). Because cutaneous-elicited responses generally are felt to be polysynaptic (Simpson 1978), this constitutes further evidence that the effects of NMDA in our experiments were due to interneuron rather than direct motoneuron activation.

The other result of this paper concerns central pattern generators (CPGs). CPGs are circuits intrinsic to the spinal cord that generate the rhythmic patterns underlying different behaviors. They may share neuronal elements or smaller unit CPGs (Grillner 1981). NMDA given systemically or intrathecally in vivo or bathing the spinal cord in vitro has been shown to activate CPGs (Dale and Roberts 1984; Douglas et al. 1993; Grillner et al. 1981; McClellan and Farel 1985). In our study, NMDA was microapplied focally and, at locations where it was effective, most commonly produced a rhythmic sequence where the forces belonged to only two or three different orientations. In addition, some rhythms were distinctly more common than others (Fig. 12). These orderly features about the rhythmic effects and the fact that they were obtained with NMDA, together suggest that they represented activation of organized rhythmic circuitry, i.e., that we locally accessed circuitries belonging to different CPGs and activated them with NMDA. We can only state this as a suggestion because the limb was not deafferented to remove peripheral feedback and because we have no behavioral correlate. Nevertheless it is interesting that in a recent investigation where NMDA was bath-applied to transverse cord slices in the presence of TTX, a subgroup of cells recorded ventrolaterally to the central canal that responded with rhythmic oscillations rather than simple depolarization was interpreted to be part of a CPG (Hochman et al. 1994a).

Analyzing the rhythmic isometric forces rather than the behaviors or the electromyograms may be providing an interesting perspective on CPGs. Indeed, it is remarkable that at our rhythmic sites, four of the five observed force orientations were the same as those of the forces obtained at the tonic sites. This strongly suggests that the different rhythms would be constructed from the simpler modules with a tonic force output.

This interpretation is further suggested by the topography (Fig. 14): each of the most common rhythms could be elicited from several distinct regions, and these were close in location to those tonic regions with an output similar to the force components of the rhythm. One exception was that the RF,FB,LE rhythm and its RF,LE subset were not elicited from a region close to the tonic RF area; however, in those rhythms, the RF was brief in contrast to the situation for the RF,FB rhythm, which in fact could be elicited from such a region. The patchy distribution of the regions from which each rhythm could be elicited (Fig. 14, *B–D*) suggests that these regions might be interconnected to constitute a network. NMDA applied to any one of these regions would in time engage the network as a whole resulting in full production of the rhythm.

The concept of a patchy rostrocaudal distribution of CPGs differs from previous studies, which have concluded either that the whole lumbosacral cord is capable of rhythmic oscillations, with the rostral segments being more rhythmogenic (Deliagina et al. 1983; Ho and O'Donovan 1993; Kjaerulff and Kiehn 1996; Mortin and Stein 1989) or that the CPG (for locomotion) is localized strictly to the uppermost two lumbar segments (Cazalets et al. 1995). On the other hand, a patchy motor organization of the spinal cord has been suggested in another context by Székely (1967) when he found on systematic microstimulation of the spinal cord in a grid-like pattern that a muscle would be activated at a certain locus in combination with some other muscles, then not be activated at the next locus, then reappear at a still farther locus in combination with a different set of muscles.

The idea that CPGs for different behaviors might be constructed from smaller units is not new. Grillner (1981) has proposed unit CPGs that might be responsible for oscillations at a single joint. The patterns of rhythmic forces that we saw were in general not those expected for such oscillations (e.g., ADD,LE or RF,CE, which would correspond to oscillations about the knee and hip joints respectively were rather rare; see Fig. 12). Our suggestion that the smaller units would be modules producing tonic forces is closer to that of Mortin and Stein (1989). They examined how the electroneurographic patterns of the three different forms of fictive scratch reflex in the turtle changed as segments were being progressively removed from the spinal cord. From this, they concluded that the same group of interneurons would be responsible for the hip protraction phase in all three scratch forms, whereas a separate group of interneurons with a different location would underlie the hip retraction phase in each case.

Although the same forces as those produced by the tonic modules were important components of the rhythms, suggesting a sequential activation of these tonic modules rather than a coactivation, the most frequent force component in rhythms, and also the strongest, was FB (flexion to body), a force not obtained tonically. Moreover FB was almost never the first force response in rhythms. Where would it arise from?

FB was the force component common to the most frequent rhythms obtained with NMDA, and comparison of their topography (Fig. 14, *B–D*) suggests that an element of the FB-generating circuitry might be the caudal zone in segment 10 from which all three of these rhythms could be elicited and which was in each case the only region that could not be linked to the other force components of these rhythms. Another possibility is that FB might have arisen through a coactivation of modules (e.g., RF and ADD), whereas the other forces represented a sequential alternating activation of the modules. Depending on the exact balance within this coactivation, one would expect

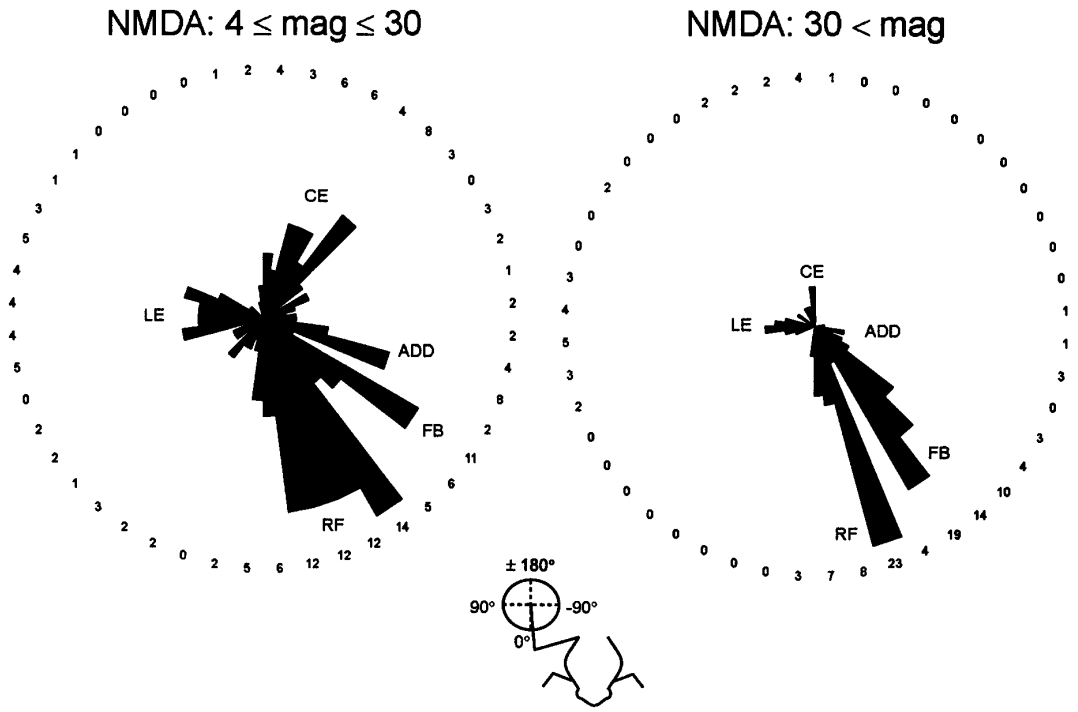

FIG. 15. Seventy-three weakest forces ($2 < \text{mag} < 4$) have been removed from the 388 NMDA-elicited forces of Fig. 6. Remaining responses have been divided in 2 groups according to force magnitude (mag), and their orientations are displayed in circular histograms. *Left*: forces with $4 \leq \text{mag} \leq 30$ ($n = 185$). Magnitude range of these forces is similar to that of the tonic responses. *Right*: forces with mag >30 ($n = 130$).

some variability in the direction of the FB vector. A related observation might be that the FB forces were more sharply distinguishable from the RF and ADD forces when the NMDA responses of Fig. 6 were subdivided into weaker and stronger ones (Figs. 15), but it is not clear how to account for this at the moment.

Coactivation by supraspinal inputs has been suggested as a means to obtain intermediate force orientations (Mussa-Ivaldi et al. 1994), but one may ask whether it could occur through purely spinal mechanisms and whether it could have another function. Spinal CPGs do not only ''pick'' force orientations but also organize them in time. A speculation would be that the tonic modules might be providing the force orientations, whereas coactivation might be more intimately related to timing. For example, all scratch forms in the turtle have strictly alternating hip protractor and retractor bursts, but it is the timing of coactivation with the knee extensor burst that crucially distinguishes between them (Stein 1983). There has been much recent work suggesting the importance of synchrony in sensory systems (König et al. 1996), but it is likely to be equally important in motor systems (Farmer 1998).

In conclusion, our findings support a modular organization of the motor system in the frog spinal cord and may provide a framework in which to investigate the hard-wired aspects of the circuitry underlying the generation of spinal cord rhythms.

We thank Dr. S. Rossignol for helpful comments on the manuscript and Dr. J. Crandall for the histology processing.

This work was supported by Office of Naval Research Grant ONR:N00014/90/J/1946 and National Institute of Neurological Disorders and Stroke Grant (NS-09343) to E. Bizzi and a Howard Hughes Medical Institute predoctoral fellowship to M. C. Tresch.

Address for reprint requests: E. Bizzi, Dept. of Brain and Cognitive Sciences, Massachusetts Institute of Technology, 77 Massachusetts Ave., E25-526, Cambridge, MA 02139.

Received 12 January 1998; accepted in final form 20 July 1998.

REFERENCES

ALFORD, S. AND GRILLNER, S. CNQX and DNQX block non-NMDA synaptic transmission but not NMDA-evoked locomotion in lamprey spinal cord. *Brain Res.* 506: 297–302, 1990.

BARRY, M. AND O'DONOVAN, M. J. The effects of excitatory amino acids and their antagonists on the generation of motor activity in the isolated chick spinal cord. *Dev. Brain Res.* 36: 271–276, 1987.

BIZZI, E., GISZTER, S. F., LOEB, E., MUSSA-IVALDI, F. A., AND SALTIEL, P. Modular organization of motor behavior in the frog's spinal cord. *Trends Neurosci.* 18: 442–446, 1995.

BIZZI, E., MUSSA-IVALDI, F. A., AND GISZTER, S. F. Computations underlying the execution of movement: a biological perspective. *Science* 253: 287–291, 1991.

CARSLAW, H. S. AND JAEGER, J. C. *Conduction of Heat in Solids.* London: Oxford, 1959.

CAZALETS, J. R., BORDE, M., AND CLARAC, F. Localization and organization of the central pattern generator for hindlimb locomotion in newborn rat. *J. Neurosci.* 15: 4943–4951, 1995.

COHEN, A. H. AND WALLÉN, P. The neuronal correlate of locomotion in fish. ''Fictive swimming'' induced in an in vitro preparation of the lamprey spinal cord. *Exp. Brain Res.* 41: 11–18, 1980.

CROSSMAN, A. R., WALKER, R. J., AND WOODRUFF, G. N. Problems associated with iontophoretic studies in the caudate nucleus and substantia nigra. *Neuropharmacology* 13: 547–552, 1974.

CURRIE, S. N. Fictive hindlimb motor patterns evoked by application of glutamate agonists to the turtle spinal cord. *Soc. Neurosci. Abstr.* 20: 1593, 1994.

CURTIS, D. R., PERRIN, D., AND WATKINS, J. C. The excitation of spinal neurones by the iontophoretic application of agents which chelate calcium. *J. Neurochem.* 6: 1–20, 1960.

DALE, N. AND ROBERTS, A. Excitatory amino acid receptors in *Xenopus* embryo spinal cord and their role in the activation of swimming. *J. Physiol. (Lond.)* 348: 527–543, 1984.

D'AVELLA, A. AND BIZZI, E. Low dimensionality of supraspinally induced force fields. *Proc. Natl. Acad. Sci. USA* 95: 7711–7714, 1998.

DAVIES, J., FRANCIS, A. A., JONES, A. W., AND WATKINS, J. C. 2-Amino-5-phosphonovalerate (2-APV), a potent and selective antagonist of amino acid-induced and synaptic excitation. *Neurosci. Lett.* 21: 77–81, 1981.

DELIAGINA, T. G., ORLOVSKY, G. N., AND PAVLOVA, G. A. The capacity for generation of rhythmic oscillations is distributed in the lumbosacral spinal cord of the cat. *Exp. Brain Res.* 53: 81–90, 1983.

DEMPSTER, A. P., LAIRD, N. M., AND RUBIN, D. B. Maximum likelihood from incomplete data via the EM algorithm. *J. R. Stat. Soc. Ser. B* 39: 1–22, 1977.

DOUGLAS, J. R., NOGA, B. R., DAI, X., AND JORDAN, L. M. The effects of intrathecal administration of excitatory amino acid agonists and antagonists on the initiation of locomotion in the adult cat. *J. Neurosci.* 13: 990–1000, 1993.

DURAND, J. NMDA actions on rat abducens motoneurons. *Eur. J. Neurosci.* 3: 621–633, 1991.

FARMER, S. F. Rhythmicity, synchronization and binding in human and primate motor systems. *J. Physiol. (Lond.)* 509: 3–14, 1998.

FISHER, N. I. *Statistical Analysis of Circular Data.* Cambridge, UK: Cambridge, 1993.

GARTHWAITE, J. Cellular uptake disguises action of L-glutamate on *N*-methyl-D-aspartate receptors. *Br. J. Pharmacol.* 85: 297–307, 1985.

GISZTER, S. F., MUSSA-IVALDI, F. A., AND BIZZI, E. Convergent force fields organized in the frog's spinal cord. *J. Neurosci.* 13: 467–491, 1993.

GRILLNER, S. Control of locomotion in bipeds, tetrapods and fish. In: *Handbook of Physiology. The Nervous System. Motor Control.* Bethesda, MD: Am. Physiol. Soc., 1981, sect. 1, vol. II, p. 1179–1236.

GRILLNER, S., BUCHANAN, J. T., WALLÉN, P., AND BRODIN, L. Neural control of locomotion in lower vertebrates: from behavior to ionic mechanisms. In: *Neural Control of Rhythmic Movements in Vertebrates,* edited by A. Cohen, S. Rossignol, and S. Grillner. New York: Wiley, 1988, p. 1–40.

GRILLNER, S., MCCLELLAN, A., SIGVARDT, K., WALLÉN, P. AND WILÉN, M. Activation of NMDA-receptors elicits ''fictive locomotion'' in lamprey spinal cord in vitro. *Acta Physiol. Scand.* 113: 549–551, 1981.

HARTIGAN, J. A. AND WONG, M. A. A k-means clustering algorithm. *Appl. Stat.* 28: 100–108, 1979.

HO, S. AND O'DONOVAN, M. J. Regionalization and intersegmental coordination of rhythm-generating networks in the spinal cord of the chick embryo. *J. Neurosci.* 13: 1354–1371, 1993.

HOCHMAN, S., JORDAN, L. M., AND MACDONALD, J. F. *N*-methyl-D-aspartate receptor-mediated voltage oscillations in neurons surrounding the central canal in slices of rat spinal cord. *J. Neurophysiol.* 72: 565–577, 1994a.

HOCHMAN, S., JORDAN, L. M., AND SCHMIDT, B. J. TTX-resistant NMDA receptor-mediated voltage oscillations in mammalian lumbar motoneurons. *J. Neurophysiol.* 72: 2559–2562, 1994b.

HOUNSGAARD, J. AND KIEHN, O. Calcium spikes and calcium plateaux evoked by differential polarization in dendrites of turtle motoneurons in vitro. *J. Physiol. (Lond.)* 486: 245–259, 1993.

HSU, Y.-S., WALKER, J. J., AND OGREN, D. E. A step-wise method for determining the number of component distributions in a mixture. *Math. Geol.* 18: 153–160, 1986.

KJAERULFF, O. AND KIEHN, O. Distribution of networks generating and coordinating locomotor activity in the neonatal rat spinal cord in vitro: a lesion study. *J. Neurosci.* 16: 5777–5794, 1996.

KÖNIG, P., ENGEL, A. K., AND SINGER, W. Integrator or coincidence detector? The role of the cortical neuron revisited. *Trends Neurosci.* 19: 130–137, 1996.

LARKUM, M. E., RIOULT, M. G., AND LÜSCHER, H. R. Propagation of action potentials in the dendrites of neurons from rat spinal cord slice cultures. *J. Neurophysiol.* 75: 154–170, 1996.

LEE, R. H. AND HECKMAN, C. J. Influence of voltage-sensitive dendritic conductances on bistable firing and effective synaptic current in cat spinal motoneurons in vivo. *J. Neurophysiol.* 76: 2107–2110, 1996.

LONGSWORTH, L. G. Diffusion measurements, at 25°C, of aqueous solutions of amino acids, peptides and sugars. *J. Am. Chem. Soc.* 75: 5705–5709, 1953.

MARDIA, K. V. *Statistics of Directional Data.* New York: Academic, 1972.

MAYER, M. L., WESTBROOK, G. L., AND VIKLICKY, L. Sites of antagonist action on *N*-methyl-D-aspartic acid receptors studied using fluctuation analysis and a rapid perfusion technique. *J. Neurophysiol.* 60: 645–663, 1988.

MCCLELLAN, A. D. AND FAREL, P. B. Pharmacological activation of locomotor patterns in larval and adult frog spinal cords. *Brain Res.* 332: 119–130, 1985.

MOORE, L. E., BUCHANAN, J. T., AND MURPHEY, C. R. Localization and interaction of *N*-methyl-D-aspartate and non-*N*-methyl-D-aspartate receptors of lamprey spinal neurons. *Biophys. J.* 68: 96–103, 1995.

MORTIN, L. I. AND STEIN, P.S.G. Spinal cord segments containing key elements of the central pattern generators for three forms of scratch reflex in the turtle. *J. Neurosci.* 9: 2285–2296, 1989.

MUSSA-IVALDI, F. A., GISZTER, S. F., AND BIZZI, E. Linear combinations of primitives in vertebrate motor control. *Proc. Natl. Acad. Sci. USA* 91: 7534–7538, 1994.

NICHOLSON, C. Diffusion from an injected volume of a substance in brain tissue with arbitrary volume fraction and tortuosity. *Brain Res.* 333: 325–329, 1985.

NICHOLSON, C., PHILLIPS, C. M., AND GARDNER-MEDWIN, A. R. Diffusion from an iontophoretic point source in the brain: role of tortuosity and volume fraction. *Brain Res.* 169: 580–584, 1979.

NICHOLSON, C. AND PHILLIPS, J. M. Ion diffusion modified by tortuosity and volume fraction in the extracellular microenvironment of the rat cerebellum. *J. Physiol. (Lond.)* 321: 225–257, 1981.

NICHOLSON, C. AND SYKOVÁ, E. Extracellular space structure revealed by diffusion analysis. *Trends Neurosci.* 21: 207–215, 1998.

PATNEAU, D. K. AND MAYER, M. L. Structure-activity relationships for amino acid transmitter candidates acting at *N*-methyl-D-aspartate and quisqualate receptors. *J. Neurosci.* 10: 2385–2399, 1990.

PETRALIA, R. S., YOKOTANI, N., AND WENTHOLD R. J. Light and electron microscope distributions of the NMDA receptor subunit NMDAR1 in the rat nervous system using a selective anti-peptide antibody. *J. Neurosci.* 14: 667–696, 1994.

POON, M. L. T. Induction of swimming in lamprey by L-DOPA and amino acids. *J. Comp. Physiol.* 136: 337–344, 1980.

RIOULT-PEDOTTI, M.-S. Intrinsic NMDA-induced oscillations in motoneurons of an adult vertebrate spinal cord are masked by inhibition. *J. Neurophysiol.* 77: 717–730, 1997.

ROBINSON, D. AND ELLENBERGER, H. Distribution of *N*-methyl-D-aspartate and non-*N*-methyl-D-aspartate glutamate receptor subunits on respiratory motor and premotor neurons in the rat. *J. Comp. Neurol.* 389: 94–116, 1997.

SEAMANS, J. K., GORELOVA, N. A., AND YANG, C. R. Contributions of voltage-gated Ca^{2+} channels in the proximal versus distal dendrites to synaptic integration in prefrontal cortical neurons. *J. Neurosci.* 17: 5936–5948, 1997.

SCHWINDT, P. C. AND CRILL, W. E. Amplification of synaptic current by persistent sodium conductance in apical dendrite of neocortical neurons. *J. Neurophysiol.* 74: 2220–2224, 1995.

SCHWINDT, P. C. AND CRILL, W. E. Local and propagated dendritic action potentials evoked by glutamate iontophoresis on rat neocortical pyramidal neurons. *J. Neurophysiol.* 77: 2466–2483, 1997.

SIMPSON, J. I. Functional synaptology of the spinal cord. In: *Frog Neurobiology. A Handbook,* edited by R. Llinas and W. Precht. Berlin: Springer-Verlag, 1978, p. 728–749.

SKYDSGAARD, M. AND HOUNSGAARD, J. Spatial integration of local transmitter responses in motoneurons of the turtle spinal cord in vitro. *J. Physiol. (Lond.)* 479: 233–246, 1994.

SOFFE, S. R. Motor patterns for two distinct rhythmic behaviors evoked by excitatory amino acid agonists in the *Xenopus* embryo spinal cord. *J. Neurophysiol.* 75: 1815–1825, 1996.

STEIN, P.S.G. The vertebrate scratch reflex. *Symp. Soc. Exp. Biol.* 37: 383–403, 1983.

STONE, T. W. The relative potencies of (−)2-amino-5-phosphonovalerate and (−)2-amino-7-phosphonoheptanoate as antagonists of *N*-methyl-aspartate and quinolinic acids and repetitive spikes in rat hippocampal slices. *Brain Res.* 381: 195–198, 1986.

STUART, G. AND SAKMANN, B. Amplification of EPSPs by axosomatic sodium channels in neocortical pyramidal neurons. *Neuron* 15: 1065–1076, 1995.

SVIRSKIS, G. AND HOUNSGAARD, J. Depolarization-induced facilitation of a plateau-generating current in ventral horn neurons in the turtle spinal cord. *J. Neurophysiol.* 78: 1740–1742, 1997.

SZÉKELY, G. Development of limb movements: embryological, physiologi-

cal and model studies. In: *Ciba Foundation Symposium on Growth of the Nervous System*, edited by G.E.W. Wolstenholme and M. O'Connor. London: Churchill, 1968, p. 77–93.

SZÉKELY, G. The morphology of motoneurons and dorsal root fibers in the frog's spinal cord. *Brain Res.* 103: 275–290, 1976.

TURNER, R. W., MALER, L., DEERINCK, T., LEVINSON, S. R., AND ELLISMAN, M. H. TTX-sensitive dendritic sodium channels underlie oscillatory discharge in a vertebrate sensory neuron. *J. Neurosci.* 14: 6453–6471, 1994.

TURNER, R. W., MEYERS, D.E.R., AND BARKER, J. L. Localization of tetrodotoxin-sensitive field potentials of CA1 pyramidal cells in the rat hippocampus. *J. Neurophysiol.* 62: 1375–1387, 1989.